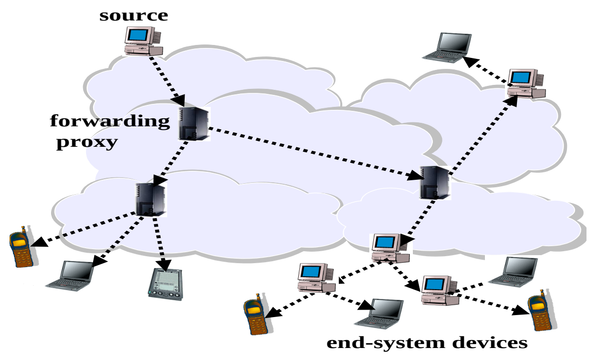

Fig. 1. Overlay Network Based Communication

packets to all the nodes in the overlay. While first metric may be a useful performance measure for non-temporal applications like long term file transfers etc., the second metric may be a useful performance measure for temporal applications (with stringent packet loss requirements) like instant messaging, secure network services, content delivery applications including streaming media for e-learning and coporate communications and mission critical data distribution.

We model the limited bandwidth of access link path of each end-system using a simple queuing model that captures the interaction between the packet processing at the incoming and outgoing interfaces. We first propose a simple bufferless queueing model and later generalize the approach for finite buffer queueing models. The bufferless model gives explicit closed form expressions for loss metrics in terms of depth of the overlay tree, the fanout of nodes, and network parameters like lode and link bandwidth. While the analysis using finite buffer model is not so explicit and expressions for loss metrics can be obtained in a recursive manner, the model is more realistic as it accounts for buffers at the input and output interfaces at end-systems and can be used to obtain queueing delays at nodes. Using the analytical results, we study the sensitivity of different loss metrics to the forwarding degree and depth of the tree.

The rest of the paper is organized as follows: Section 2 introduces two different performance metrics for packet loss. In Section 3 we motivate the queueing model and derive explicit expressions for loss at an individual node. We derive expressions for the m-ary overlay tree for different metrics for packet loss in Section 4. Section 5 illustrates the numerical results based on our analysis and studies the sensitivity of overlay perfromance. Section 6 summarizes the results and discusses our ongoing future works.

2 Application Specific Performance Metrics for Packet Loss

Figure 1 illustrates a motivational application scenario deployed in the Internet using overlay network. We shall be concerned with packet loss in this study to show how different metric for packet loss may influence the construction of an overlay network and assume delay to be dominated by propagation delay over links and (assuming the nodes to be in reasonable proximity) is given in terms of the hop count. The finitness of the buffers allows us to account for queueing delays at overlay nodes. The study involving queueing delay in addition to propagation delay is the subject of our ongoing work. We define the follwoing performance metrics:

- c_1: minimizing c_1 amounts to maximizing the fraction of packets that are correctly received by the worst node (the worst node being the one with the largest end to end packet loss probability).

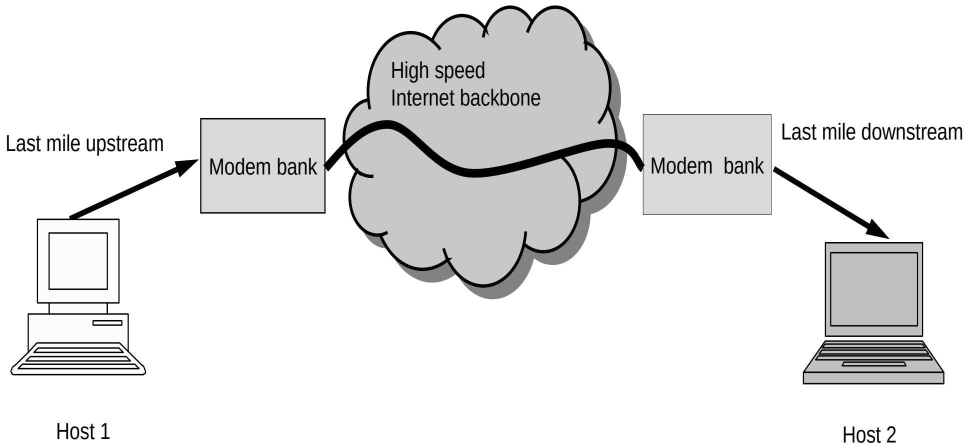

Fig. 2. Various components in an end-to-end path

- c_2: minimizing c_2 amounts to maximizing the expected delivery of all packets to all the nodes in the overlay.

Next we mathematically characterize these metrics. Let us consider the case of transmission of application packets by the source node to a group of $N-1$ nodes. For the ith node we define the random variable $Y_i(n)$ as: $Y_i(n) = 1(0)$, if the nth packet is received by node i (otherwise). Define $\tilde{Y}_i(n) = 1 - Y_i(n)$. We consider $\{\tilde{Y}_i(n), n \geq 1\}$ to be i.i.d. (the distribution we shall determine in our analysis).

- $c_1 = \max_i E[\tilde{Y}_i] = \max_i p_i$, where p_i is the probability that the packet is not received by node i [1]. Thus minimizing c_1 amounts to minimizing the loss probability of the worst node.
- $c_2 = E[\max_i \tilde{Y}_i]$: minimizing c_2 loss amounts to maximizing the probability of correct delivery of each packet to each node. This is an important metric for temporal, mission-critical group communication applications where its highly desirable that all the nodes are receiving all the information.

Observe that $c_1 < c_2$ (by Jensen's inequality), thus c_2 is a much stringent loss requirement.

3 Queueing Model to Capture Access Link Sharing

Figure 2 illustrates the various components involved in the forwarding of data from one host to another using overlay network. First host 1 sends data to its output interface, which is transmitted to the (DSL/Cable/Dialup) access hub using the uplink. The access hub forwards to the other end over the high speed Internet that is received at host 2's (DSL/Cable/Dialup) access hub. This data is then forwarded to host 2 on its "last mile" downstream link.

We consider the queueing model depicted in Figure 3 to abstract different components in the data forwarding path in an overlay. The first queue represents forwarding over the upstream link that is shared across all the data forwarding paths from host 1 to its children nodes. We approximate the service rate available to one receiving host (in this case host 2) as r_{out}/m, where m is the forwarding degree of host 1. We also assume that a B_{out} amount of buffer is allocated for buffering data in the kernel/device for forwarding data on this stream. The next service station with infinite server model accounts for the propagation delay from one access hub to the other end of the access hub over the Internet. There is no queueing and loss at this station as the Internet is order of magnitude faster compared to the last mile. Next queue with service rate r_{in} represents the forwarding from access hub to the host 2 over the downstream last mile link. The queue in host 2 represents the processing overhead with service rate u_s and buffer capacity B_{in} at the input interface of host 2.

Given that the processing overhead is much smaller compared to the forwarding rate on the outgoing interface, we represent each node with a single queue with a buffer size $K \equiv B_{in}+B_{out}$ with the processing

[1] p_i is basically the loss probability of the path from the source to the i node

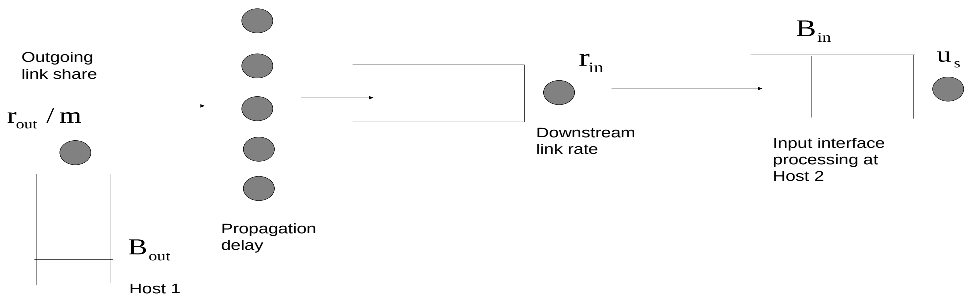

Fig. 3. Modeling end-to-end path

rate r/m (with r being the link bandwidth and $r \approx r_{out}$). We consider the problem in a homogeneous setting for analytical tractability, i.e., each node has same forwarding capacity and forwarding fanout of every node is assumed to be same for every participating nodes. Thus we limit our illustrations to regular m-ary tree configuration for overlay network topology. Let d be the depth of a topology and N represent the number of end-system nodes in the overlay network. We represent the end-to-end delay as the number of hops from the source to the destination node. Note that we are concerned with regular m-trees in our analysis. An $m-$tree is characterized by a constant branching ratio of m and the depth of the tree is the smallest integer d that satisfies:

$$N \leq 1 + m + m^2 + \ldots + m^d$$

Thus $d = \lceil \frac{\ln(N(m-1)+1)}{\ln m} - 1 \rceil$ when the delay is expressed as the hop distance

Fig. 4 shows a $m = 2$ tree with $N = 3$. As illustrated in Figure 4, the arrival process at the downstream node is thinned due to losses at upstream nodes. Let the input arrival rate to node A is λ and p is the loss probability of a data unit at A. By *flow conservation* the average departure rate from A is $\lambda(1-p)$. Thus its children B_1 and B_2 will each have the average input arrival rates as $\lambda(1-p)$.

3.1 Bufferless Model: Loss and Delay Expressions

We first *approximate* the network of nodes between the source and the leaf node as a tandem of $M/M/1$ queues with zero buffer. We take the mean size of a packet as $1/\mu$. If a node has m children and the node bandwidth is shared in a processor sharing manner (at packet level) we approximate the service rate at each of the m connections by r/m. Thus the mean service time of a packet is $\frac{m}{r\mu}$. In this approximation the input to queue 0 is Poisson with rate $\lambda_0 \equiv \lambda$, to queue 1 is Poisson with rate $\lambda_1 \equiv \lambda(1 - P_0)$ and similarly the input to queue j is Poisson with rate $\lambda_j \equiv \lambda \Pi_{k=0}^{j-1}(1 - P_k)$, where P_k is the loss probability at a bufferless $M/M/1$ queue (representing the kth node in the path between a node and the root node) with arrival rate $\lambda \Pi_{s=0}^{k-1}(1 - P_s)$ and service rate $\frac{\mu r}{m}$. Let $\rho = \frac{\lambda}{\mu r}$.

By simple $M/M/1$ formulation with zero buffer the loss probability of a packet at node 0 is given by:

$$P_0 = \frac{m\rho}{1 + m\rho}.$$

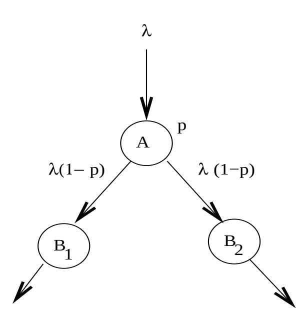

Fig. 4. A $m = 2$ tree with $N = 3$.

In general for $0 \le j \le d$, we get

$$P_j = \frac{m\rho}{1+(j+1)m\rho}. \tag{1}$$

Observe that because of symmetry, the loss probability at all nodes at level j is given by P_j, $0 \le j \le d$.

3.2 Finite Buffer Model: Loss and Delay Expressions

To capture the finiteness of the buffers at overlay node and hence the packet losses and queueing delays at the overlay nodes we model a node as $M/M/1/K$ queue instead of bufferless as in the previous model. Again we approximate the input to queue 0 as Poisson with rate $\lambda_0 \equiv \lambda$, to queue 1 Poisson with rate $\lambda_1 \equiv \lambda(1-\pi_0)$ and similarly the input to queue j is Poisson with rate $\lambda_j \equiv \lambda \Pi_{k=0}^{j-1}(1-\pi_k)$, where π_k is the loss probability at a $M/M/1/K$ queue (representing the kth node) with arrival rate $\lambda \Pi_{i=0}^{k-1}(1-\pi_i)$ and service rate $\frac{\mu r}{m}$. From queueing theory, we have $\pi_0 = \frac{(m\rho)^K}{\sum_{j=0}^{K}(m\rho)^j}$. The expressions for π_j, $1 \le j \le d$ can be obtained similarly by accounting for losses at upstream nodes.

4 Expressions for Different Performance Metrics

We shall obtain expressions for c_1 and c_2 using the loss probability relations obtained in previous section. We shall restrict our analysis to bufferless model and obtain explicit closed form expressions.

4.1 Expression for c_1

With any packet we associate at each node j, $0 \le j \le d$, in tandem, an indicator function $\bar{X}_j$. $\bar{X}_j = 0$ if the packet is lost at the j node and is 1 otherwise. Also given $\bar{X}_{j-1} = 0$ we take $\bar{X}_i = 0, i \ge j$ [2]. From our analysis we get $E[\bar{X}_0] = (1-P_0)$, $E[\bar{X}_1|\bar{X}_0 = 1] = (1-P_1)$ and in general $E[\bar{X}_j|\bar{X}_i = 1, 1 \le i \le j-1] = (1-P_j)$, where P_js are given by (1). Let $\bar{p}(j)$ be the probability that a packet is received at a node at depth j, $0 \le j \le d$, [3]. $\bar{p}(0)$ is probability that a packet is not lost at the root node in an m-tree. We have $\bar{p}(0) = 1 - P_0 \equiv \frac{1}{1+m\rho}$. $\bar{p}(1)$ is given by:

$$\bar{p}(1) = P(\bar{X}_0 = 1, \bar{X}_1 = 1) = E[\bar{X}_0]E[\bar{X}_1|\bar{X}_0 = 1] = (1-P_0)(1-P_1) = \frac{1}{1+2m\rho}$$

Continuing this way, the probability that a packet correctly reaches a node at depth d is given by

$$\begin{aligned}\bar{p}(d) &= E[\bar{X}_0]E[\bar{X}_1|\bar{X}_0 = 1]E[\bar{X}_2|\bar{X}_2 = 1, \bar{X}_1 = 1]\dots \\ &\quad \dots E[\bar{X}_d|\bar{X}_0 = 1, \bar{X}_1 = 1, \dots, \bar{X}_{d-1} = 1] \\ &= (1-P_0)(1-P_1)\dots(1-P_d) = \frac{1}{1+(d+1)m\rho}\end{aligned} \tag{2}$$

Thus the maximum end-to-end loss probability (as a function of m and d), $p(d) \stackrel{\text{def}}{=} 1 - \bar{p}(d)$, is $\frac{(d+1)m\rho}{1+(d+1)m\rho}$. For a complete tree $d + 1 = \frac{\ln(N(m-1)+1)}{\ln m}$.

Since it is an $m-$tree, all leaf nodes at depth d (this is the same as all leaf nodes if its a regular $m-$tree) will have same probability that a packet from the root will reach them correctly. Thus to calculate $c_1 := \max_{1 \le i \le N} p_i$, we look at the end-to-end loss probability seen by the leaf nodes and hence c_1 is simply the end-to-end loss probability from the source to any of the leaf nodes, given by:

$$c_1 = \frac{1}{1 + \left(m\rho \frac{\ln(N(m-1)+1)}{\ln m}\right)^{-1}} \tag{3}$$

[2] This is because if the packet is lost at an upstream node it will never reach the downstream node as so is considered to be lost at downstreams nodes.

[3] We assume that a packet is received at any node j correctly if it is not lost at node j and at any of the succesive upstream nodes in the path from the root till node j.

4.2 Expression for c_2

To calculate c_2 we first obtain the distribution of $\max_{i=\{1,2,\ldots,N\}} \tilde{Y}_i$. Observe that $\tilde{Y}_i = \tilde{Y}_{i-1} + (1-\tilde{Y}_{i-1})X_i$. Thus we have $\max(\tilde{Y}_i, \tilde{Y_{i-1}}) = \tilde{Y}_i$. Continuing in this way we shall observe that $\max_{i=\{1,2,\ldots,N\}} \tilde{Y}_i = \max_{j=\{N-m^d, N-m^d+1,\ldots,N\}} \tilde{Y}_i$, i.e., we should only look at the max over set of leaf nodes. To make the analysis simple, we shall first obtain the expression for c_2 for a binary tree with depth 2 and later generalize it to any $m-ary$ tree with depth d. Thus we will first obtain the distribution of $\max_{i=1,\ldots,7} \tilde{Y}_i$. Let random variable $X_i = 1 - \bar{X}_i$ for $i = 1, \ldots, 7$, From our analysis in previous section, we have $p_1 \equiv P_0$, $p_2 = p_3 \equiv P_2$, $p_4 = p_5 = p_6 = p_7 \equiv P_3$. After some algebra we get:

$$\begin{aligned}
\max_{i=\{1,\ldots,7\}} \tilde{Y}_i &= \max\left(\tilde{Y}_4, \tilde{Y}_5, \tilde{Y}_6, \tilde{Y}_7\right) \\
&= \max\left(X_1 + (1-X_1)X_2 + (1-X_1)(1-X_2)\max(X_4, X_5), X_1 + (1-X_1)X_3\right. \\
&\quad \left. +(1-X_1)(1-X_3)\max(X_6, X_7)\right) \\
&= \max\left(X_1 + (1-X_1)X_2 + (1-X_1)(1-X_2)Z_2^{(1)},\right. \\
&\quad \left. X_1 + (1-X_1)X_3 + (1-X_1)(1-X_3)Z_2^{(2)}\right) \\
&= X_1 + (1-X_1)\left(\max\left(X_2 + (1-X_2)Z_2^{(1)}, X_3 + (1-X_3)Z_2^{(2)}\right)\right) = X_1 + (1-X_1)Z_1^{(1)},
\end{aligned}$$

where $Z_2^{(1)} = \max(X_4, X_5)$, $Z_2^{(2)} = \max(X_6, X_7)$ and $Z_1^{(1)} = \max\left(X_2 + (1-X_2)Z_2^{(1)}, X_3 + (1-X_3)Z_2^{(2)}\right)$. Observe that all the random variables are binary valued taking 0 or 1 values. Thus $E[\max_i \tilde{Y}_i] = E[X_1 + (1-X_1)E[Z_1^{(1)}|X_1 = 0]$. We shall next find the conditional distribution of $Z_1^{(1)}$ given $X_1 = 0$. This requires finding the conditional distribution of $\max\left(X_2 + (1-X_2)Z_2^{(1)}, X_3 + (1-X_3)Z_2^{(2)}\right)$ given $X_1 = 0$. We shall first find the conditional expectation of random variables $X_2 + (1-X_2)Z_2^{(1)}$ and $X_3 + (1-X_3)Z_2^{(2)}$ given $X_1 = 0$. Observe that

$$E[X_2 + (1-X_2)Z_2^{(1)}|X_1 = 0] = p_2 + (1-p_2)E[Z_2^{(1)}|X_1 = 0, X_2 = 0] \tag{4}$$

Similarly we have:

$$E[X_3 + (1-X_3)Z_2^{(2)}|X_1 = 0] = p_3 + (1-p_3)E[Z_2^{(2)}|X_1 = 0, X_3 = 0] \tag{5}$$

Further we have $E[Z_2^{(1)}|X_1 = 0, X_2 = 0] = E[\max(X_4, X_5)|X_1 = 0, X_2 = 0]$. We shall next find the conditional distribution of X_4 and X_5 given $X_1 = 0$ and $X_2 = 0$. We have:

$$P(X_4 = 1|X_1 = 0, X_2 = 0) = p_4 = 1 - P(X_4 = 0|X_1 = 0, X_2 = 0) \tag{6}$$

Similarly we have:

$$P(X_5 = 1|X_1 = 0, X_2 = 0) = p_5 = 1 - P(X_5 = 0|X_1 = 0, X_2 = 0) \tag{7}$$

Thus we have from (6) and (7):

$$E[Z_2^{(1)}|X_1 = 0, X_2 = 0] = 1 - (1-p_4)(1-p_5). \tag{8}$$

Which implies from (4) and (8):

$$E[X_2 + (1-X_2)Z_2^{(1)}|X_1 = 0] = p_2 + (1-p_2)(1-(1-p_4)(1-p_5)), \tag{9}$$

and similarly we can obtain from (5) and (8):

$$E[X_3 + (1-X_3)Z_2^{(2)}|X_1 = 0] = p_3 + (1-p_3)(1-(1-p_6)(1-p_7)). \tag{10}$$

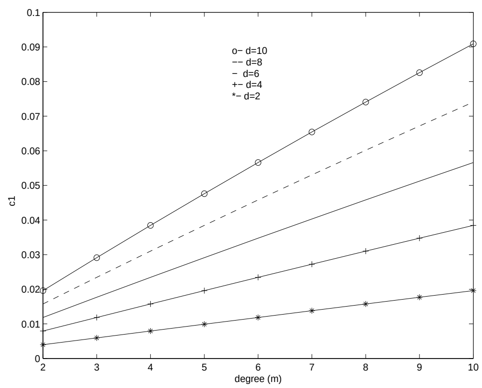

Fig. 5. c_1 as a function of the forwarding degree and depth of the tree for $\rho = 0.001$ with the bufferless model.

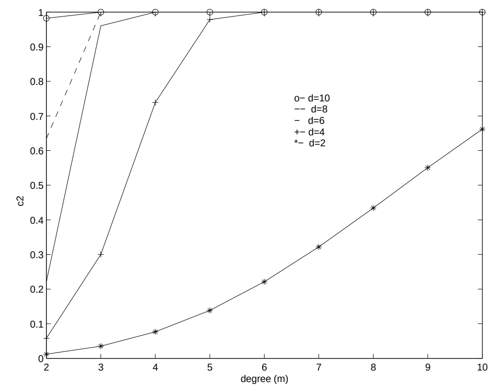

Fig. 6. c_2 as a function of the forwarding degree and depth of the tree for $\rho = 0.001$ with the bufferless model.

Thus we have

$$E[Z_1^{(1)}|X_1 = 0] = 1 - (1-p_2)(1-p_3)(1-p_4)(1-p_5)(1-p_6)(1-p_7).$$

Hence, $E[\max_i \tilde{Y}_i] = p_1 + (1-p_1)(1-(1-p_2)(1-p_3)(1-p_4)(1-p_5)(1-p_6)(1-p_7)) = 1 - \prod_{i=1}^{7}(1-p_i)$. Observe that, from our analysis we have, $p_2 = p_3 = P_1 = \frac{m\rho}{1+2m\rho}$ and $p_4 = p_5 = p_6 = p_7 = P_2 = \frac{m\rho}{1+3m\rho}$. In general, for any set of nodes at depth j [4], the probability that a packet is lost at that node, given the packet is not lost at any of its successive nodes in the tree is $P_j \equiv \frac{m\rho}{1+(j+1)m\rho}$. Let $v(j)$ be the number of nodes that have the same depth j for $j \le d$. For a complete $m-ary$ tree we have, for any $0 \le j \le d$: $v(j) = m^j$. Thus we get:

$$E[\max_i \tilde{Y}_i] = 1 - \prod_{i=1}^{7}(1-p_i) = 1 - \prod_{j=0}^{2}(1-P_j)^{v(j)} \tag{11}$$

The symmetry of the results suggests that the arguments can be generalized to an $m-ary$ tree with depth d. Thus we have

$$\max_i Y_i = \begin{cases} 1 \text{ w.p. } 1 - \prod_{j=0}^{d}(1-P_j)^{v(j)} = 1 - \prod_{j=0}^{d}\left(\frac{1+jm\rho}{1+(j+1)m\rho}\right)^{m^j} \\ 0 \text{ w.p. } \prod_{j=0}^{d}\left(\frac{1+jm\rho}{1+(j+1)m\rho}\right)^{m^j} \end{cases} \tag{12}$$

From (12) we have: $c_2 = 1 - \prod_{j=0}^{d}\left(\frac{1+jm\rho}{1+(j+1)m\rho}\right)^{m^j}$.

5 Numerical Studies

We first plot c_1 and c_2 as a function of the depth d and forwarding degree m of the tree for $\rho = 0.001$ in Figs. 5 and 6 respectively and further in Figs. 7 and 8 for $\rho = 0.01$. We quantitatively study the maximum number of users that can be supported in the overlay $N_{max}\left(= \frac{m^{d+1}-1}{m^d-1}\right)$, if the bounds on c_1 and c_2 are relaxed. Table 1 shows that relative increase in the maximum number of nodes that can be supported as c_1 and c_2 bounds are relaxed for $d = 4$ and $\rho = 0.001$. From the Table we observe that for a given depth as c_1 is relaxed from 0.0079 to 0.039, $N_{\max}$ increases from 31 to 1111. The gain is more significant for large d as we observe from Fig. 5, as d increases the slope of the c_1 vs. m curve increases.

Since c_2 is a much stringent requirement as the degree of the tree is increased to support a large population of users (see Table 1 and Fig. 6 and 8) the degradation in c_2 is quite significant as compared

[4] Here the root node is at depth 0 and the leaf nodes are at depth d.

m	$N_{\max}$	c_1	c_2
2	31	0.0099	0.0579
3	121	0.0148	0.300
4	341	0.0196	0.7389
5	781	0.0244	0.9785
6	1555	0.0291	0.9999
10	1111	0.0476	1.000

Table 1. Table showing the relative increase in the maximum number of nodes that can be supported as c_1 and c_2 bounds are relaxed for $d = 4$.

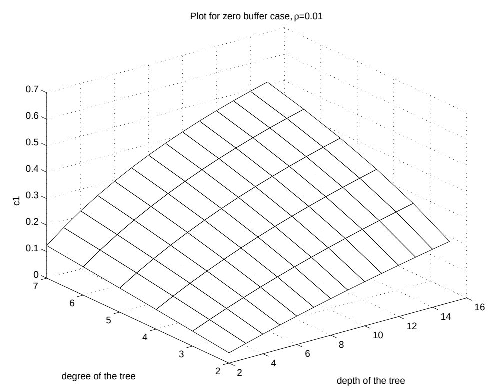

Fig. 7. The gain in $N_{\max}$ $\left(= \frac{m^{d+1}-1}{m^d-1}\right)$ with the relaxation in c_1 for bufferless model with $\rho = 0.01$.

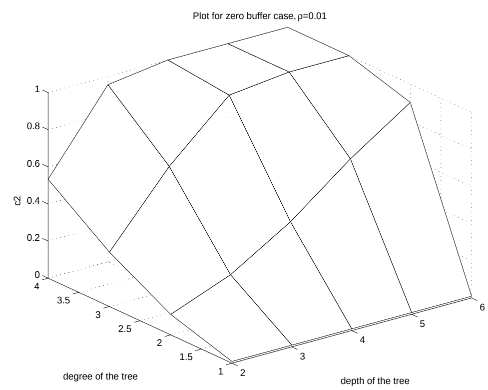

Fig. 8. The gain in $N_{\max}$ $\left(= \frac{m^{d+1}-1}{m^d-1}\right)$ with the relaxation in c_2 for bufferless model with $\rho = 0.01$.

to the degradation in c_1. An interesting observation is that as the depth of the trees increases c_2 increases quite sharply as compared to c_1 suggesting that increasing the depth of the tree so as to increase the population of supported nodes might potentially violate the performance requirement of applications and the adverse effects are more severe on c_2 as compared to c_1

We next plot similar curves for the finite buffer model by using our analytical results in Fig 9 and Fig. 10 for c_1 and c_2 respectively. The trends are similar to curves with bufferless model.

5.1 Network Simulations: Model Validation and Robustness

To validate our mathematical models and its assumptions we created a discrete event simulator. The simulator allows the creation of arbitrary networks of buffered nodes, exponential and deterministic service processes for packet forwarding, several packet arrival processes (Poisson, Markov Modulated Poisson (MMPP), and Constant Bit Rate (CBR)), and various network latency delays. Each node has its own buffer and input/output interfaces to its neighbors in the overlay, and all events occur according to a common timeline.

Each simulation data point reported represents an average over 10 or more simulation runs (with different random seeds), and with 10,000 packets sent per run. All simulations use a network size of 10,000 nodes. Figure 11 compares c_1 from the analysis and the simulation results for the Poisson arrival case with different load and node buffer size. We observe that *our assumptions on the arrivals into the subsequent nodes in the overlay being Poisson match very closely with the simulation results*.

Figure 12 illustrates the robustness of our model with MMPP arrival process for $\rho = 0.5, 0.1$. We compare the value of c_1 with MMPP arrival process obtained via simulation with the analysis using the Poisson arrival process. The arrival rate of the Poisson process is taken equal to the mean arrival rate of the MMPP process. We find a good match between simulation results for MMPP and our analysis with Poisson arrival.

Typically applications have loss and/or delay requirements and an overlay supporting the application should be constructed such that it meets the loss and dealy bounds while supporitng the application. To

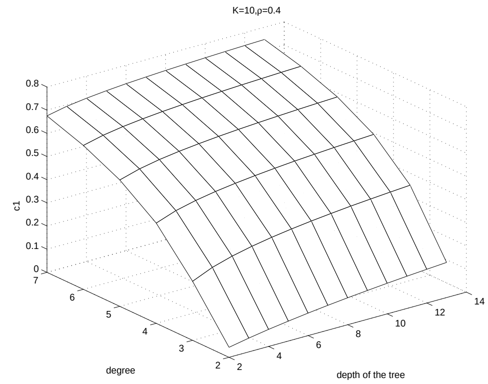

Fig. 9. The gain in m with the relaxation in c_1 for a given depth for the finite buffer, $K = 10$, $\rho = 0.4$.

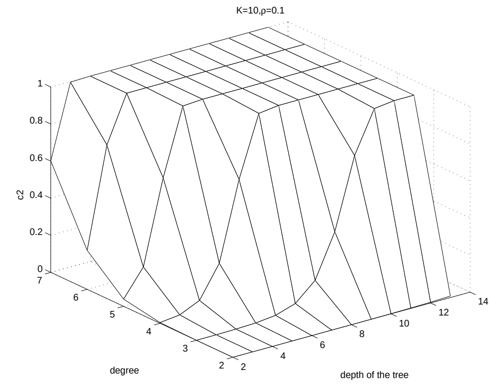

Fig. 10. The gain in m with the relaxation in c_2 for a given depth for the finite buffer, $K = 20$, $\rho = 0.1$.

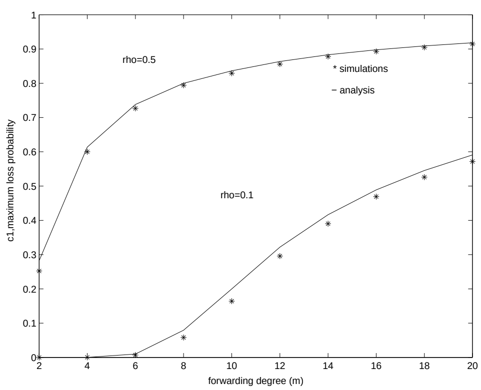

Fig. 11. Model validation, $\rho = 0.1, 0.5$, $K = 6$

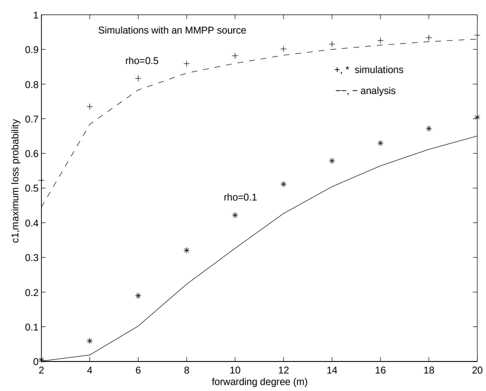

Fig. 12. Model robustness with MMPP arrival process with finite buffers, $K = 6$.

capture this, we next define the concept of a *feasible set of forwarding degree* of the tree. A feasible set of forwarding degree is a set, $\tilde{M} = \{\tilde{m}\}$ of degrees such that a regular tree constructed with degree $\tilde{m} \in \tilde{M}$ satisfies the loss and/or delay bounds. We next study the robustness of our model with different packet size distribution and arrival process. In particualr we are interested in identifying the set $\tilde{M}$ of feasible degree for different scenarios such that the constructed tree satifies bounds on c_1 and end to end delay (hop count).

Approach	$\mathcal{P}_\beta$	$\mathcal{D}_\Delta$	$\mathcal{P}_\beta \bigcap \mathcal{D}_\Delta$
Model Analysis	(2,4,...,10)	(2,4,...,12)	(2,4,...,10)
Poisson Simuls.	(2,4,...,10)	(2,4,...,12)	(2,4,...,10)
MMPP Simuls.	(2,4,...,10)	(2,4,...,12)	(2,4,...,10)
On-off CBR Simuls.	(2,4,...,20)	(2,4,...,12)	(2,4,...,10)

Table 2. The set of feasible degrees obtained from analysis and from simulations using different arrival processes and packet size distribution.

We consider three arrival processes, i.e., Poisson, MMPP and on-off CBR arrival at the origin source. We take c_1 bound (β) to be 0.35, and delay bound (Δ) as 6, and $\rho = 0.1$. Table 2 illustrates the set of feasible degrees for loss bound ($\mathcal{P}_\beta$), for delay bound ($\mathcal{D}_\Delta$), and that meets both the loss and delay bounds ($\mathcal{P}_\beta \bigcap \mathcal{D}_\Delta$). We find that our model is able to predict the feasible degree of the overlay quite accurately for the MMPP and CBR case. *We observe that for arrival processes other than Poisson (and* *loss rate for MMPP), the exact values of maximum delay and loss do not match very closely with our simple model. However, we find that feasible value of the forwarding degree for the homogeneous case is relatively insensitive to the exact statistics of the arrival process* and/or the packet size distribution. This is an important result as our simple model can be used as a guideline for constructing overlay even for more complicated arrival processes.

6 Conclusions

In this study, we provided a theoretical framework for understanding the impact of different performance metrics for packet loss on the overlay network construction. We identified two broad classes of performance metrics catering to different application-specific QoS requirements. Using simple queing models, we derived explicit expressions for these loss metrics in terms of the tree topology (forwarding degree, depth) and network parameters (load, link bandwidth, node buffers).

Using the analytical results, we studied the sensitivity of different loss metrics to the forwarding degree and depth of the tree. We observe different trends in the packet loss metrics as a function of the depth of the tree for a given forwarding degree of the node. Also we observe that as the degree of the nodes is increased to support a larger number of end-system nodes, the degradation in c_2 is quite significant as compared to that in c_1. These trends indicate that one has to construct an overlay tree differently based on application specific metrics. Our observations based on our analysis and numerical results provide useful design insights for constructing overlays meeting application specific performance requirements.

In this paper, we have focussed on the different performance metrics for the packet loss. However observe that the finiteness of the buffer at the nodes adds to the end-to-end queuing delay which was approximated by the hop count in the paper. Depending on the tree topology and the network load, the queuing delay can be a significant component of the end-to-end delay. We are presently studying the tradeoff between the end-to-end delay (including queueing delays) and loss metrics within our framework, which will potentially provide us guidelines for choosing the appropriate forwarding degree to support both delay and loss sensitive applications.

References

1. S. Banerjee, C. Kommareddy, K. Kar, B. Bhattacharjee, S. Kuller, *Construction of an Efficient Overlay Multicast Infrastructure for Real-Time Applicatons*, in Proceedings of IEEE Infocom 2003.
2. S. Banerjee, S. Lee, B. Bhattacharjee, A. Srinivasan, *Resilient Multicast Using Overlay*, ACM Sigmetrics, 2003.
3. Y.-H. Chu, S. G. Rao, and H. Zhang, *A Case for End System Multicast*, in Proceedings of ACM SIGMETRICS, June 2000.
4. J. Jannotti, D. Gifford, K. Johnson, M. Kaashoek, and J. O'Toole, *Overcast: Reliable Multicasting with an Overlay Network*, in Proceedings of the 4th Symposium on Operating Systems Design and Implementation, Oct. 2000.
5. N. Malouch, Z. Liu, D. Rubenstein, S. Sahu, *A Graph Theoretic Approach to Bounding Delay in Proxy-Assisted, End-system Multicast*, Proc. of Tenth International Workshop on Quality of Service (IwQoS 2002).
6. S. Shi and J. S. Turner, *Multicast Routing and Bandwidth Dimensioning in Overlay Networks*, IEEE JSAC (2002).